Annals of Nuclear Medicine (2018) 32:256–263
https://doi.org/10.1007/s12149-018-1240-5

ORIGINAL ARTICLE

^{18}F-FPYBF-2, a new F-18 labelled amyloid imaging PET tracer: biodistribution and radiation dosimetry assessment of first-in-man ^{18}F-FPYBF-2 PET imaging

Ryuichi Nishii[1,2] · Tatsuya Higashi[1,2] · Shinya Kagawa[1] · Chio Okuyama[1] · Yoshihiko Kishibe[1] · Masaaki Takahashi[1] · Tomoko Okina[3] · Norio Suzuki[3] · Hiroshi Hasegawa[3] · Yasuhiro Nagahama[4] · Koichi Ishizu[2,5] · Naoya Oishi[6] · Hiroyuki Kimura[7] · Hiroyuki Watanabe[8] · Masahiro Ono[8] · Hideo Saji[8] · Hiroshi Yamauchi[1]

Received: 9 February 2018 / Accepted: 12 February 2018 / Published online: 16 February 2018

Abstract

Objective Recently, a benzofuran derivative for the imaging of β-amyloid plaques, 5-(5-(2-(2-(2-^{18}F-fluoroethoxy)ethoxy)ethoxy)benzofuran-2-yl)- *N*-methylpyridin-2-amine (^{18}F-FPYBF-2) has been validated as a tracer for amyloid imaging and it was found that ^{18}F-FPYBF-2 PET/CT is a useful and reliable diagnostic tool for the evaluation of AD (Higashi et al. Ann Nucl Med, https://doi.org/10.1007/s12149-018-1236-1, 2018). The aim of this study was to assess the biodistribution and radiation dosimetry of diagnostic dosages of ^{18}F-FPYBF-2 in normal healthy volunteers as a first-in-man study.

Methods Four normal healthy volunteers (male: 3, female: 1; mean age: 40 ± 17; age range 25–56) were included and underwent ^{18}F-FPYBF-2 PET/CT study for the evaluation of radiation exposure and pharmacokinetics. A 10-min dynamic PET/CT scan of the body (chest and abdomen) was performed at 0–10 min and a 15-min whole-body static scan was performed six times after the injection of ^{18}F-FPYBF-2. After reconstructing PET and CT image data, individual organ time–activity curves were estimated by fitting volume of interest data from the dynamic scan and whole-body scans. The OLINDA/EXM version 2.0 software was used to determine the whole-body effective doses.

Results Dynamic PET imaging demonstrated that the hepatobiliary and renal systems were the principal pathways of clearance of ^{18}F-FPYBF-2. High uptake in the liver and the gall bladder, the stomach, and the kidneys were demonstrated, followed by the intestines and the urinary bladder. The ED for the adult dosimetric model was estimated to be 8.48 ± 1.25 μSv/MBq. The higher absorbed doses were estimated for the liver (28.98 ± 12.49 and 36.21 ± 15.64 μGy/MBq), the brain (20.93 ± 4.56 and 23.05 ± 5.03μ Gy/MBq), the osteogenic cells (9.67 ± 1.67 and 10.29 ± 1.70 μGy/MBq), the small intestines (9.12 ± 2.61 and 11.12 ± 3.15 μGy/MBq), and the kidneys (7.81 ± 2.62 and 8.71 ± 2.90 μGy/MBq) for male and female, respectively.

Conclusions The ED for the adult dosimetric model was similar to those of other agents used for amyloid PET imaging. The diagnostic dosage of 185–370 MBq of ^{18}F-FPYBF-2 was considered to be acceptable for administration in patients as a diagnostic tool for the evaluation of AD.

Keywords Alzheimer disease · Amyloid imaging · Normal healthy volunteers · Positron emission tomography · Biodistributtion · Radiation dosimetry · OLINDA/EXM

Introduction

For diagnosing Alzheimer's disease (AD) which is the most common neurodegenerative disorder and the most common cause of dementia in the elderly with steadily increasing numbers [1], the ability to detect deposition of amyloid beta (Aβ) protein is an area of active research in molecular imaging. Developing imaging probes to evaluate amyloid deposition is an ongoing pursuit that could be helpful in the diagnosis of AD. Several imaging tracers,

This study is registered in UMIN Clinical Trials Registry (UMIN-CTR) as UMIN study ID: UMIN000010304, UMIN000012297, and UMIN000012299.

Electronic supplementary material The online version of this article (https://doi.org/10.1007/s12149-018-1240-5) contains supplementary material, which is available to authorized users.

✉ Tatsuya Higashi
higashi.tatsuya@qst.go.jp

Extended author information available on the last page of the article

especially for positron emission tomography (PET), has been developed and reported to evaluate amyloid deposition, such as ^{11}C-Pittsburgh compound B (PiB) [2], ^{11}C-BF227 [3], ^{18}F-AZD4694 [4], ^{18}F-FACT [5], ^{18}F-BAY-949172 (^{18}F-florbetaben) [6], ^{18}F-AV-45 (^{18}F-florbetapir) [7], and ^{18}F-GE067 (^{18}F-Flutemetamol) [8]. PiB, the first amyloid imaging PET tracer, has been reported with successful results and used widely as a research tool [9].

Recently, we developed a benzofuran derivative for the imaging of Aβ protein, 5-(5-(2-(2-(2-^{18}F-fluoroethoxy)ethoxy)ethoxy)benzofuran-2-yl)- *N*-methylpyridin-2-amine (^{18}F-FPYBF-2) [10, 11]. This new fluorinated benzofuran derivative, which is like ^{18}F-AZD4694 but has a fluoropolyethylene glycol side chain, is promising PET probes for cerebral Aβ plaques imaging, and the specific labeling of Aβ plaques was observed in autoradiographic sections of autopsied AD brain. It should be noted that ^{18}F-FPYBF-2 has a stable chemical structure which does not photodegrade. ^{18}F-FPYBF-2 is a ^{18}F-labeled analog, which has the much longer half-life of ^{18}F ($t1/2 = 110$ min), should offer a more manageable manufacturing and delivery process for clinical practice, as compared to ^{11}C labeled tracers.

In a clinical setting using healthy volunteers and patients with dementia, ^{18}F-FPYBF-2 has been already validated as a tracer for amyloid imaging and it was found that ^{18}F-FPYBF-2 PET/CT is a useful and reliable diagnostic tool for the evaluation of AD [12]. However, evaluation regarding biodistribution of ^{18}F-FPYBF-2 and radiation dosimetry of ^{18}F-FPYBF-2 PET imaging were not assessed and reported to the full.

Therefore, to facilitate clinical application of ^{18}F-FPYBF-2 PET/CT, we have conducted studies aimed at assessing the biodistribution and radiation dosimetry of diagnostic dosages of ^{18}F-FPYBF-2 in normal healthy volunteers as a first-in-man study.

Materials and methods

Automated radiosynthesis and preparation of ^{18}F-FPYBF-2

^{18}F-FPYBF-2 was prepared in-house as described before [12]. Briefly, the ^{18}F-fluoride was produced with a cyclotron, CYPRIS HM18 (Sumitomo Heavy Industries (SHI), Ltd., Japan) by the ^{18}O(p, n)^{18}F reaction on 98% enriched ^{18}O water. The radiosynthesis of ^{18}F-FPYBF-2 was performed using a modification of the methods described by Ono et al. [10] and on a hybrid synthesizer, cassette-type multipurpose automatic synthesizer module (JFE Engineering Corporation, Japan).

Normal healthy volunteers

From March 2013 to October 2017, normal healthy volunteers were recruited for this dynamic PET study and finally 4 normal healthy volunteers (male: 3, female: 1; mean age: 40 ± 17; age range 25–56) (Table 1) were included and underwent ^{18}F-FPYBF-2 PET/CT study for the evaluation of radiation exposure and pharmacokinetics. Eligibility criteria for healthy volunteers (20 years old or older) in the present study were follows; 1) who did not give any subjective complaint about cognitive problem, and (2.1) who made a declaration of their healthy status without medication, or (2.2) who had underlying non-neurological illness, such as hypertension, diabetes, hyperlipidemia, but controlled them well by medication as an out-patient based medical practice. Exclusion criteria were follows; (1) who had a subjective complaint or objective symptom of cognitive problem, (2) who were treated with or had past history of neurological disorder and related diseases, (3) who were treated with or had past history of brain or head injury. Each volunteer gave a written informed consent form defined by our institutional review boards with the information about the expected radiation exposure. The tracer study for normal healthy volunteers was approved by our institutional review boards, the Human Study Committee (approved on Mar. 28, 2013) and the Committee for the Clinical Use of Short-Half Life Radioactive Materials (approved on Mar. 1, 2013), where our protocol was investigated according to the results of animal studies of safety performed in 2012 as an extended single intravenous dose toxicity study, which was based on the protocol of Guidance for the Performing of Microdose Clinical Trials announced by the Ministry of Health, Labour and Welware of Japan.

PET/CT data acquisition

In first-in-man volunteer study for newly developed ^{18}F-FPYBF-2, all normal healthy volunteers underwent ^{18}F-FPYBF-2 PET/CT. PET/CT scans were performed by a whole-body PET/CT scanner, Siemens True Point Biograph 16 (pixel size: 1.34 mm) (Siemens/CTI, Erlangen,

Table 1 Profile of normal healthy volunteers and injected radioactivity of ^{18}F-FPYBF-2

Subjects	Gender	Age	Injected dose (MBq)
#1 (TTT)	Male	53	199
#2 (AAA)	Male	26	236
#3 (KKK)	Male	25	220
#4 (HHH)	Female	56	199
Mean ± SD		40 ± 17	213 ± 18

Germany) after the intravenous injection of ^{18}F-FPYBF-2 (213 ± 18 MBq). A 10-minutes dynamic PET/CT scan of the body (chest and abdomen) was performed at 0–10 min and a 15-minutes whole-body static scan was performed six times; 15–30, 30–45, 45–60, 60–75, 75–90 and 90–105 min, after the injection of ^{18}F-FPYBF-2. For the image data processing in PET/CT scanner, the trans-axial effective field of view of the scanner was 342 mm in diameter, and the matrix size was 256 × 256. All acquisition data were reconstructed by 2 iterations and 21 subsets by the PET/CT scanner, using the three-dimensional ordered subset expectation maximization, OS-EM. The CT data were used for attenuation correction.

Imaging analysis

Regional dynamic and whole-body reconstructed PET and CT data were stored in the DICOM file format and were analyzed using PMOD software version 3.3 (PMOD Technologies Ltd., Zurich, Switzerland). Three-dimensional volumes of interest (VOIs) of individual source organs were constructed on the PET images to include all organ activity. The following source organs, the heart, aorta (blood), lung, liver, gallbladder, kidneys, pancreas, spleen, vertebral bone, muscle, small intestine, large intestine were analyzed for dynamic images. For the whole-body image analysis, the brain and salivary glands, urinary bladder, and whole body in addition to the above organ were analyzed. VOIs were manually drawn and corrected around the tissues referring CT images and mean activity concentration was expressed as Bq/cm^3. Tissue distribution in organs of ^{18}F-FPYBF-2 expressed SUV was plotted against time to obtain time-activity curves (TACs) of measured organs.

Time-integrated activity coefficient and absorbed radiation dose Calculations

Individual organ time–activity curves were estimated by fitting volume of interest data from the dynamic scan and whole-body scans for the four subjects. The whole-body time–activity curves were constructed by taking the activity in the entire whole-body (including the urinary bladder) in the first 3 whole-body scans and decay-correcting them to the time of administration. This was assumed to represent the entirety of the administered activity. The remaining 2 whole-body scans were constructed by taking the activity in the entire whole body excluding those of the urinary bladder at the time of the third whole-body scan, assuming a 1-h voiding interval to estimate the residence time of urine in the bladder. Radiation absorbed doses and effective doses were calculated based on the RADAR method [13] using OLINDA/EXM2.0 software (HERMES Medical Solutions and Vanderbilt University, Stockholm Sweden) [14, 15]. The time-integrated activity coefficient (formerly called the residence time) was calculated by dividing the fractional uptake parameter of the exponential fit to the original data (not corrected for decay) by the decay constant of the fit. Each organ volume obtained by the PET/CT images was converted to organ masses according to the International Commission on Radiological Protection Publication 89 (ICRP-89) male and female phantom-models [16]. Organ absorbed doses and effective dose (ED) per absorbed activity in μGy/MBq and μSv/MBq, were calculated, respectively, using the ICRP-103 tissue weighting factors [17].

Statistics

All values are expressed as mean ± SD. All the statistical analysis was performed using statistical software, JMP 8J version.

Results

PET imaging of pharmacokinetics and biodistribution of ^{18}F-FPYBF-2

None of the subjects injected with 213 ± 18 MBq of ^{18}F-FPYBF-2 demonstrated observable adverse events or clinically detectable pharmacologic effects, and any apparent changes in standard vital signs during three months follow-up period. Dynamic PET imaging demonstrated that the hepatobiliary and renal systems were the principal pathways of clearance of ^{18}F-FPYBF-2 (Fig. 1). High uptake in the liver and the gall bladder, the stomach, and the kidneys were demonstrated, followed by the intestines and the urinary bladder. Some accumulation of ^{18}F-FPYBF-2 was observed in the brain (Table 2). No significant accumulation or retention of ^{18}F-FPYBF-2 was observed in the lung, the genital organs. There were mild depositions of radioactivity in the skeletal structures, the muscle, salivary glands. The time-activity curves of ^{18}F-FPYBF-2 radioactivity concentration in different organs and tissues were determined from PET/CT images (Fig. 2). Within 1 min, the level of radioactivity in the aorta (blood) reached SUVmax; 12.6 ± 5.34 and then cleared bi-exponentially with the fast phase between 1 and 10 min and then a slow phase until 90 min. Accumulation of the radioactivity into the liver and kidney was observed, reaching concentrations of SUVmax; 9.29 ± 1.60 at 10 min and SUVmax; 13.12 ± 52.13 at 1 min, respectively. There was a relatively low level of uptake in the lung, the pancreas, the spleen and the muscle throughout the 90 min of the study.

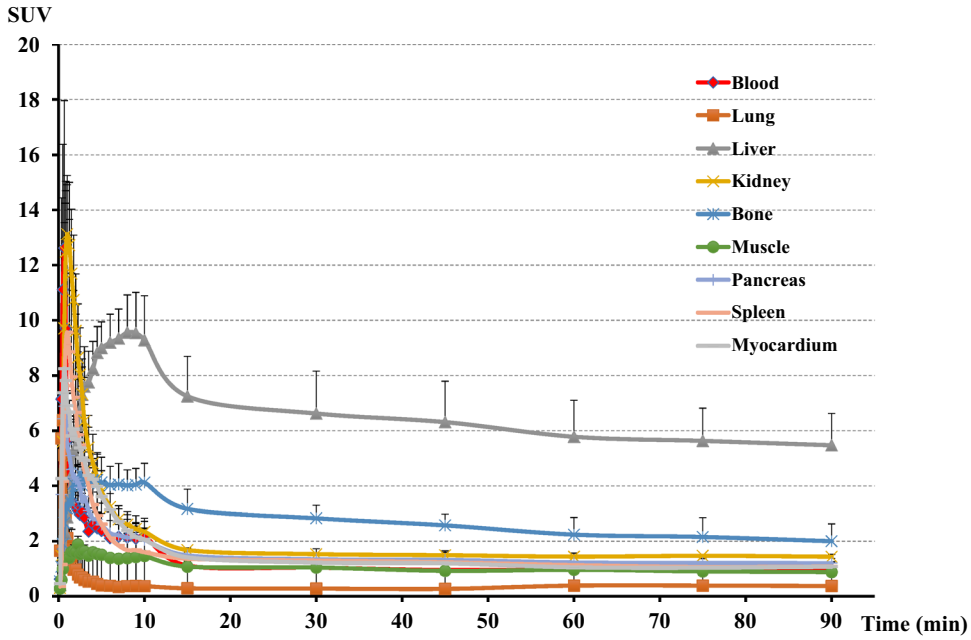

Fig. 1 Time-activity curve of ^{18}F-FPYBF-2 uptake (SUV) in selected organs and tissues determined from dynamic and whole-body PET images of four normal healthy volunteers. Data were expressed in mean ± s.d

Table 2 Uptake of ^{18}F-FPYBF-2 in the Brain obtained from whole-body PET images of four normal healthy volunteers

Time (min)	15	30	45	60	75	90
Blood (Aorta)	1.12 ± 0.20	1.05 ± 0.17	0.95 ± 0.15	0.98 ± 0.16	0.95 ± 0.16	0.92 ± 0.12
Brain (Cortex)	1.68 ± 0.31	1.57 ± 0.33	1.48 ± 0.28	1.35 ± 0.27	1.33 ± 0.22	1.21 ± 0.19

Radiation dosimetry

To assess human radiation exposure due to diagnostic dosages of ^{18}F-FPYBF-2, the radiation absorbed doses to organs were estimated using organ time-integrated activity coefficients from each individual (Table 3). The mean organ doses and EDs normalized to the unit-injected activity applied to ICRP-89 male and female phantom models are given in Table 4 and 5. The ED for the adult dosimetric model was estimated to be 8.48 ± 1.25 μSv/MBq (3.14 ± 0.46 mSv/370 MBq). The higher absorbed doses were estimated for the liver (28.98 ± 12.49 and 36.21 ± 15.64 μGy/MBq), the brain (20.93 ± 4.56 and 23.05 ± 5.03μ Gy/MBq), the osteogenic cells (9.67 ± 1.67 and 10.29 ± 1.70 μGy/MBq), the small intestines (9.12 ± 2.61 and 11.12 ± 3.15 μGy/MBq), and the kidneys (7.81 ± 2.62 and 8.71 ± 2.90 μGy/MBq) for male and female, respectively.

Discussion

This study was conducted to facilitate the clinical imaging study with ^{18}F-FPYBF-2, a benzofuran derivative for the imaging of Aβ protein. Previously, ^{18}F-FPYBF-2 showed high binding affinity for Aβ aggregates in ex-vivo autoradiograms of brain sections from Tg2576 mice and for amyloid plaques in sections of autopsied AD brain [10]. Recently, we reported the usefulness of ^{18}F-FPYBF-2 imaging for the evaluation of AD [12]. In that study, static head PET image acquisition for 20-minutes was performed 50–70 min after the intravenous injection of ^{18}F-FPYBF-2 (200 ± 22 MBq).

In this first-in-man study, the pattern of biodistribution and clearance of ^{18}F-FPYBF-2 were similar to those reported before in mice study [10]. ^{18}F-FPYBF-2 was mainly excreted by the liver and substantial intestinal discharge of the radioactive material was observed. This radiotracer also showed considerable renal excretion. The slight uptake in the brain in normal healthy volunteers was observed from the early phase after the injection of ^{18}F-FPYBF-2, which was supposed to be suitable for neuro imaging for diagnosis of AD.

Based on the results of the present study in normal healthy volunteers, the estimated ED in human patients after administration of 185–370 MBq of ^{18}F-FPYBF-2 is 1.57–3.14 mSv (8.48 ± 1.25 μSv/MBq). Previous studies of ^{11}C-PiB PET imaging showed ED estimation (Adult Phantom Model) as 4.74 μSv/MBq [18] or 5.29 μSv/MBq [19]. As anticipated, whole-body ED for ^{18}F-FPYBF-2 was greater than those for ^{11}C-PiB because of the longer decay

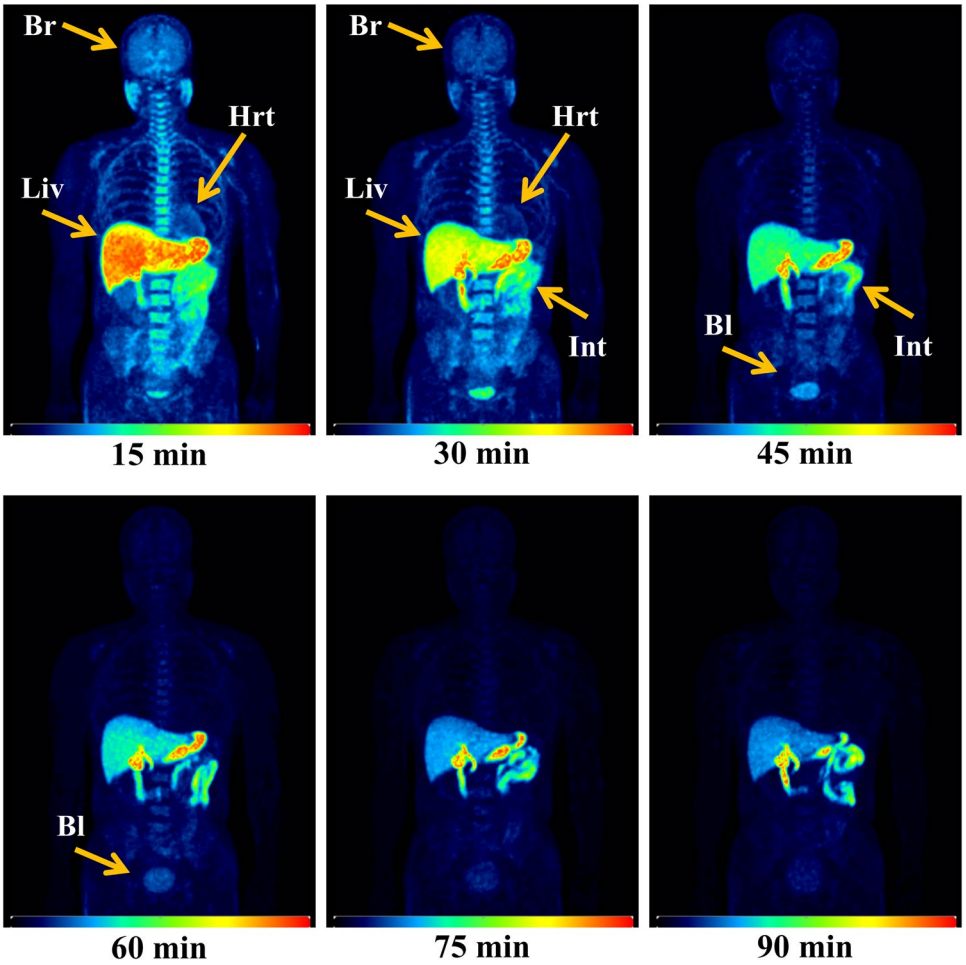

Fig. 2 Representative whole-body coronal maximum intensity projection (MIP) PET images obtained at 15, 30, 45, 60, 75 and 90 min. Different organs are indicated by arrows and labeled as; *Br* brain, *Hrt* heart, *Liv* liver, *Int* intestine, *Bl* urinary bladder

Table 3 Time-integrated activity coefficients of each organ calculated from biodistribution data of FPYBF2 in healthy subjects

Organ	#1 (TTT)	#2 (AAA)	#3 (KKK)	#4 (HHH)	Mean	S.D.
Brain	1.18E−01	1.16E−01	1.70E−01	1.05E−01	1.27.E−01	2.91.E−02
Gallbladder Wall	1.72E−03	1.52E−03	1.69E−03	2.65E−03	1.90.E−03	5.11.E−04
Small Intestine	1.33E−01	1.88E−01	1.45E−01	2.58E−01	1.81.E−01	5.65.E−02
Right colon	1.86E−02	1.26E−02	1.01E−02	1.19E−02	1.33.E−02	3.69.E−03
Heart Contents	1.85E−02	1.82E−02	1.70E−02	1.90E−02	1.82.E−02	8.50.E−04
Heart Wall	1.45E−02	1.03E−02	1.07E−02	1.76E−02	1.33.E−02	3.45.E−03
Kidneys	2.28E−01	1.28E−01	1.98E−01	1.07E−01	1.65.E−01	5.71.E−02
Liver	3.30E−01	1.16E−01	1.53E−01	1.90E−01	1.97.E−01	9.35.E−02
Lungs	1.16E−02	1.23E−02	1.85E−02	1.05E−02	1.32.E−02	3.59.E−03
Pancreas	1.35E−02	1.88E−02	1.05E−02	9.62E−03	1.31.E−02	4.14.E−03
Trabecular Bone	1.75E−01	1.82E−01	1.06E−01	1.24E−01	1.47.E−01	3.75.E−02
Spleen	1.00E−02	1.05E−02	1.31E−02	1.39E−02	1.19.E−02	1.92.E−03
Urinary Bladder Contents	5.57E−03	1.19E−02	1.33E−02	1.21E−02	1.07.E−02	3.49.E−03

half-life of ^{18}F ($t1/2 = 110$ min) than of ^{11}C ($t1/2 = 20$ min). In ^{11}C-PiB PET imaging study, however, patients usually supposed to receive a relatively higher radioactive dose of ^{11}C-PiB (i.e. 555 MBq) to obtain appropriate image quality. Thus, it implies that ED of ^{11}C-PiB PET imaging in a clinical setting is around 2.6 to 2.9 mSv. Therefore, the radiation exposure of ^{18}F-FPYBF-2 PET can be considered allowable for clinical PET study for dementia. Concerning the radiation exposure of other amyloid imaging agents, the estimated EDs were reported as follows; 14.67 μSv/MBq for

Table 4 Mean organ absorbed doses to the ICRP 89 adult (a) male and (b) female phantom model in OLINDA/EXM 2.0 using time-integrated activity coefficients from normal healthy volunteers after intravenous injection of ^{18}F-FPYBF-2

Organ	#1 (TTT)	#2 (AAA)	#3 (KKK)	#4 (HHH)	(μGy/MBq) Mean ± SD	mGy/370 MBq Mean ± SD
(a)						
Adrenals	1.93	1.08	1.47	1.13	1.40 ± 0.39	0.52 ± 0.14
Brain	19.60	19.20	27.60	17.30	20.93 ± 4.56	7.74 ± 1.69
Esophagus	5.20	3.30	3.63	3.90	4.01 ± 0.83	1.48 ± 0.31
Gallbladder wall	1.41	0.76	0.88	1.12	1.04 ± 0.28	0.39 ± 0.11
Left colon	3.19	3.05	2.83	3.58	3.16 ± 0.31	1.17 ± 0.12
Small intestine	7.00	9.38	7.38	12.70	9.12 ± 2.61	3.37 ± 0.96
Stomach wall	5.98	4.38	4.42	4.72	4.87 ± 0.76	1.80 ± 0.28
Right colon	7.23	5.00	4.46	5.31	5.50 ± 1.21	2.04 ± 0.45
Rectum	0.53	0.60	0.52	0.72	0.59 ± 0.09	0.22 ± 0.03
Heart wall	1.26	0.93	0.95	1.28	1.10 ± 0.19	0.41 ± 0.07
Kidneys	10.75	6.07	9.25	5.19	7.81 ± 2.62	2.89 ± 0.97
Liver	46.75	18.10	23.33	27.75	28.98 ± 12.49	10.72 ± 4.62
Lungs	5.53	3.98	5.03	4.26	4.70 ± 0.71	1.74 ± 0.26
Pancreas	2.00	2.36	1.55	1.60	1.88 ± 0.38	0.69 ± 0.14
Prostate	0.09	0.09	0.08	0.10	0.09 ± 0.01	0.03 ± 0.00
Salivary glands	2.34	2.24	2.90	1.97	3.36 ± 0.39	0.87 ± 0.14
Red marrow	7.97	7.28	5.50	6.71	6.86 ± 1.04	2.54 ± 0.39
Osteogenic cells	10.50	10.30	7.18	10.70	9.67 ± 1.67	3.58 ± 0.62
Spleen	1.45	1.30	1.63	1.60	1.50 ± 0.15	0.55 ± 0.06
Testes	0.22	0.24	0.20	0.22	0.22 ± 0.02	0.08 ± 0.01
Thymus	0.23	0.16	0.17	0.20	0.19 ± 0.03	0.07 ± 0.01
Thyroid	1.51	1.17	1.23	1.14	1.26 ± 0.17	0.47 ± 0.06
Urinary bladder wall	3.975	7.025	7.55	7.35	6.48 ± 1.68	2.40 ± 0.62
(b)						
Adrenals	1.78	1.03	1.33	1.12	1.31 ± 0.33	0.49 ± 0.12
Brain	21.60	21.20	30.40	19.00	23.05 ± 5.03	8.53 ± 1.86
Breasts	1.93	1.23	1.31	1.44	1.48 ± 0.32	0.55 ± 0.12
Esophagus	7.13	4.18	4.70	5.08	5.27 ± 1.29	1.95 ± 0.48
Gallbladder wall	1.53	1.01	1.16	1.33	1.26 ± 0.23	0.47 ± 0.08
Left colon	2.84	2.52	2.46	3.00	2.70 ± 0.26	1.00 ± 0.10
Small intestine	8.58	11.42	9.02	15.46	11.12 ± 3.15	4.11 ± 1.17
Stomach wall	7.14	5.46	5.68	6.22	6.12 ± 0.75	2.27 ± 0.28
Right colon	7.23	5.29	4.81	5.66	5.75 ± 1.05	2.13 ± 0.39
Rectum	0.45	0.52	0.47	0.59	0.51 ± 0.06	0.19 ± 0.02
Heart wall	1.46	1.13	1.14	1.54	1.32 ± 0.21	0.49 ± 0.08
Kidneys	12.00	6.78	10.25	5.83	8.71 ± 2.90	3.22 ± 1.07
Liver	58.50	22.60	29.25	34.50	36.21 ± 15.64	13.40 ± 5.79
Lungs	6.58	4.76	6.05	5.05	5.61 ± 0.85	2.08 ± 0.31
Ovaries	1.71	1.85	1.63	2.24	1.86 ± 0.27	0.69 ± 0.10
Pancreas	2.54	2.78	1.92	1.93	2.29 ± 0.44	0.85 ± 0.16
Salivary glands	2.64	2.53	3.24	2.23	2.66 ± 0.42	0.98 ± 0.16
Red marrow	10.08	9.33	6.88	8.67	8.74 ± 1.37	3.23 ± 0.51
Osteogenic cells	11.20	10.90	7.76	11.30	10.29 ± 1.70	3.81 ± 0.63
Spleen	1.83	1.61	2.03	1.95	1.85 ± 0.18	0.69 ± 0.07
Thymus	0.25	0.18	0.19	0.21	0.20 ± 0.03	0.08 ± 0.01
Thyroid	1.79	1.39	1.47	1.35	1.50 ± 0.20	0.55 ± 0.07
Urinary bladder wall	4.83	8.50	9.00	9.03	7.84 ± 2.02	2.90 ± 0.75
Uterus	0.15	0.18	0.15	0.22	0.17 ± 0.03	0.06 ± 0.01

Table 5 Effective doses to the ICRP 89 adult female phantom model in OLINDA/EXM 2.0 using time-integrated activity coefficients from normal healthy volunteers after intravenous injection of ^{18}F-FPYBF-2

Effective dose	#1 (TTT)	#2 (AAA)	#3 (KKK)	#4 (HHH)	Mean ± SD
(μSv/MBq)	10.30	7.46	7.93	8.23	8.48 ± 1.25
(mSv/370MBq)	3.81	2.76	2.93	3.05	3.14 ± 0.46

^{18}F-BAY94-9172 [19], 18.0 μSv/MBq for ^{18}F-AV-45 [20], and 33.8 μSv/MBq for ^{18}F-GE067 [21]. It was considered that our study protocol with the 1-hour voiding interval in this study may result in lower ED value of ^{18}F-FPYBF-2 PET study than those of other PET studies. Therefore, as for the radiation exposure control of patients, urination before and after scan should be encouraged.

The critical organs for ^{18}F-FPYBF-2 were the liver, kidneys, and the brain which are relatively high uptake organs of this radiotracer. Intestines were also one of critical organ, which is due to combined radiation exposure from the surrounding organs such as the liver, kidney, and urinary bladder. For comparison, the reported radiation absorbed doses after the administration of ^{11}C-PiB in humans were 19.0-19.88 μGy/MBq in the liver, 3.10–3.92 μGy/MBq in the brain, 12.6-12.92 μGy/MBq in the kidneys,3.62–4.65 μGy/MBq in the small intestine [18, 19]. Furthermore, the reported radiation absorbed doses after the administration of ^{18}F-AV-45 in 3 humans were 44.4 μGy/MBq in the liver, 13.8 μGy/MBq in the brain, 16.6 μGy/MBq in the kidneys, 55.2 μGy/MBq in the small intestine [20]. These results suggest that the diagnostic dosage of 185–370 MBq of ^{18}F-FPYBF-2 may be acceptable for administration in human patients and that its radiation exposure is well below the limit of 50 mSv per organ per year, which is set forth in the FDA regulations (21 CFR 361.1) [22–24].

Our clinical study with healthy volunteer and dementia patients clearly indicated that ^{18}F-FPYBF-2 is a safe amyloid PET tracer with longer half-life with F-18 and is comparable to ^{11}C-PiB in the detectability of amyloid deposition [12]. In this report, PET study with healthy volunteers showed that ^{18}F-FPYBF-2 uptake was mainly observed in cerebral white matter and that average Mean Cortical Index was low and stable basically independent from age or gender. In patients with AD, ^{18}F-FPYBF-2 uptake was observed both in cerebral white and gray matter and Mean Cortical Index was significantly higher than those of volunteers and other dementia. In comparative study, the results of 18F-FPYBF-2 PET/CT were comparable with those of 11C-PiB, and the Mean Cortical Index showed direct proportional relationship with each other. Although ^{18}F-FPYBF-2 is a "late" amyloid PET tracer after the appearance of several tracers in clinical practice with comparable diagnostic ability, we would like to show the potential of ^{18}F-FPYBF-2 as diagnostic abilities as an amyloid imaging tracer and expand the utilization of this tracer further in various fields of research and clinical practice.

There are several issues in terms of the study limitation. First, the pharmacokinetics and metabolic analysis of ^{18}F-FPYBF-2 were not determined in this present study, however another report about those data is in preparation. Second, the present first-in-man study reports for the radiation dosimetry assessment of ^{18}F-FPYBF-2 PET imaging using recently released OLINDA/EXM version 2.0 [14] implemented the RADAR (Radiation Dose Assessment Resource) method, which is conceptually the same as the MIRD method and is a U.S. FDA approved software tool. Since previously reported dosimetric data used for comparison in this study were calculated by former version of OLINDA/EXM 1.0 or 1.1, those data might be slightly different from present results, and the direct comparison might not be appropriate. But this version 2.0 is reported to adopts the modified algorithm to the previous version 1.0 and 1.1 to match the organ masses shown in ICRP publication 89 [16].

Conclusions

The radiation dosimetry for amyloid imaging agents ^{18}F-FPYBF-2 was determined in this first-in-man study. The ED for the adult dosimetric model is 8.48 ± 1.25 μSv/MBq that is similar to those of other agents used for amyloid PET imaging. The diagnostic dosage of 185–370 MBq of ^{8}F-FPYBF-2 is considered to be acceptable for administration in patients as a diagnostic tool for the evaluation of Alzheimer's disease.

Acknowledgements This work was supported by the Japan Society for the Promotion of Science (JSPS) through the "Funding Program for Next Generation World-Leading Researchers (NEXT Program, LS060)," initiated by the Council for Science and Technology Policy (CSTP).

Compliance with ethical standards

Conflict of interest No potential conflicts of interest were disclosed with regard to this study.

References

1. Alzheimer Disease International. World Alzheimer Report 2016. 2016. https://www.alz.co.uk/research/WorldAlzheimerReport2016.pdf. Accessed 9 July 2017.
2. Mathis C, Wang Y, Holt D, Huang G, Debnath M, Klunk W. Synthesis and evaluation of 11C-labeled 6-substituted 2-arylbenzothiazoles as amyloid imaging agents. J Med Chem. 2003;46:2740–54.
3. Kudo Y, Okamura N, Furumoto S, Tashiro M, Furukawa K, Maruyama M, et al. 2-(2-[2-Dimethylaminothiazol-5-yl]Ethenyl)-6-(2-[Fluoro]Ethoxy) Benzoxazole: a novel PET agent for in vivo detection of dense amyloid plaques in Alzheimer's disease patients. J Nucl Med. 2007;48:553 – 61.
4. Juréus A, Swahn BM, Sandell J, Jeppsson F, Johnson AE, Johnström P, et al. Characterization of AZD4694, a novel fluorinated Abeta plaque neuroimaging PET radioligand. J Neurochem. 2010;114:784 – 94.
5. Furumoto S, Okamura N, Furukawa K, Tashiro M, Ishikawa Y, Sugi K, et al. A 18F-labeled BF-227 derivative as a potential radioligand for imaging dense amyloid plaques by positron emission tomography. Mol Imaging Biol. 2013;15:497–506.
6. Rowe CC, Ackerman U, Browne W, Mulligan R, Pike KL, O'Keefe G, et al. Imaging of amyloid beta in Alzheimer's disease with 18F-BAY94-9172, a novel PET tracer: proof of mechanism. Lancet Neurol. 2008;7:129 – 35.
7. Choi SR, Golding G, Zhuang Z, Zhang W, Lim N, Hefti F, et al. Preclinical properties of 18F-AV-45: a PET agent for Abeta plaques in the brain. J Nucl Med. 2009;50:1887–94.
8. Nelissen N, Van Laere K, Thurfjell L, Owenius R, Vandenbulcke M, Koole M, et al. Phase 1 study of the Pittsburgh compound B derivative 18F-flutemetamol in healthy volunteers and patients with probable Alzheimer disease. J Nucl Med. 2009;50:1251–9.
9. Vandenberghe R, Adamczuk K, Dupont P, Laere KV, Chételat G. Amyloid PET in clinical practice: Its place in the multidimensional space of Alzheimer's disease. Neuroimage Clin. 2013;2:497–511.
10. Ono M, Cheng Y, Kimura H, Cui M, Kagawa S, Nishii R, et al. Novel 18F-labeled benzofuran derivatives with improved properties for positron emission tomography (PET) imaging of β-amyloid plaques in Alzheimer's brains. J Med Chem. 2011;54:2971–9.
11. Cheng Y, Ono M, Kimura H, Kagawa S, Nishii R, Saji H. A novel 18F-labeled pyridyl benzofuran derivative for imaging of beta-amyloid plaques in Alzheimer's brains. Bioorg Med Chem Lett. 2010;20:6141–4.
12. Higashi T, Nishii R, Kagawa S, Kishibe Y, Takahashi M, Okina T, et al. 18F-FPYBF-2, a new F-18 labelled amyloid imaging PET tracer - First-in-man volunteer study and clinical evaluation of patients with dementia. Ann Nucl Med. 2018. https://doi.org/10.1007/s12149-018-1236-1.
13. Stabin MG, Siegel JA. Physical models and dose factors for use in internal dose assessment. Health Phys. 2003;85:294–310.
14. Stabin MG, Siegel JA. RADAR Dose Estimate Report: A Compendium of Radiopharmaceutical Dose Estimates Based on OLINDA/EXM Version 2.0. J Nucl Med. 2018;59:154–160.
15. Stabin MG, Sparks RB, Crowe E. OLINDA/EXM: the second-generation personal computer software for internal dose assessment in nuclear medicine. J Nucl Med. 2005;46:1023–7.
16. ICRP, 2002. Basic anatomical and physiological data for use in radiological protection reference values. ICRP Publication 89. Ann ICRP 32 (3–4).
17. ICRP, 2007. The 2007 Recommendations of the International Commission on Radiological Protection. ICRP Publication 103. Ann ICRP 37 (2–4).
18. Scheinin NM, Tolvanen TK, Wilson IA, Arponen EM, Nagren KA, Rinne JO. Biodistribution and radiation dosimetry of the amyloid imaging agent 11C-PIB in humans. J Nucl Med. 2007;48:128 – 33.
19. O'Keefe GJ, Saunder TH, Ng S, Ackerman U, Tochon-Danguy HJ, Chan JG, et al. Radiation dosimetry of beta-amyloid tracers 11C-PiB and 18F-BAY94-9172. J Nucl Med. 2009;50:309 – 15.
20. Lin KJ, Hsu WC, Hsiao IT, Wey SP, Jin LW, Skovronsky D, et al. Whole-body biodistribution and brain PET imaging with [18F] AV-45, a novel amyloid imaging agent—a pilot study. Nucl Med Biol. 2010;37:497–508.
21. Koole M, Lewis DM, Buckley C, Nelissen N, Vandenbulcke M, Brooks DJ, et al. Whole-body biodistribution and radiation dosimetry of 18F-GE067: a radioligand for in vivo brain amyloid imaging. J Nucl Med. 2009;50:818 – 22.
22. ICRP Radiation dose to patients from radiopharmaceuticals: a compendium of current information related to frequently used substances. 2015. ICRP Publication 128. Ann. ICRP 44(2S).
23. Kase K. Radiation protection principles of NCRP. Health Phys. 2004;87:251–7.
24. Macey D, Williams L, Breitz H, Liu A, Johnson T, Zanzonico P. A primer for radioimmunotherapy and radionuclide therapy. AAPM Rep. 2001;71. https://www.aapm.org/pubs/reports/rpt_71.pdf.

Affiliations

Ryuichi Nishii[1,2] · Tatsuya Higashi[1,2] · Shinya Kagawa[1] · Chio Okuyama[1] · Yoshihiko Kishibe[1] · Masaaki Takahashi[1] · Tomoko Okina[3] · Norio Suzuki[3] · Hiroshi Hasegawa[3] · Yasuhiro Nagahama[4] · Koichi Ishizu[2,5] · Naoya Oishi[6] · Hiroyuki Kimura[7] · Hiroyuki Watanabe[8] · Masahiro Ono[8] · Hideo Saji[8] · Hiroshi Yamauchi[1]

1 Shiga Medical Center Research Institute, Moriyama, Japan

2 Dept. of Molecular Imaging and Theranostics, National Institute of Radiological Sciences (NIRS), National Institutes for Quantum and Radiological Science and Technology (QST), Chiba, Japan

3 Dept. of Geriatric Medicine, Shiga General Hospital, Moriyama, Japan

4 Kawasaki Memorial Hospital, Kawasaki, Japan

5 Human Health Sciences, Graduate School of Medicine, Kyoto University, Kyoto, Japan

6 Research and Educational Unit of Leaders for Integrated Medical System, Center for the Promotion of Interdisciplinary Education and Research, Kyoto University, Kyoto, Japan

7 Dept. of Analytical and Bioinorganic Chemistry, Kyoto Pharmaceutical University, Kyoto, Japan

8 Dept. of Patho-Functional Bioanalysis, Graduate School of Pharmaceutical Sciences, Kyoto University, Kyoto, Japan